

Reactions of Iron(III) Porphyrins with Oxidants. Structure–Reactivity Studies

Teddy G. Traylor,*[†] Cheal Kim, Joseph L. Richards, Feng Xu, and Charles L. Perrin*

Contribution from the Department of Chemistry-0358, University of California at San Diego, 9500 Gilman Drive, La Jolla, California 92093–0358

Received March 7, 1994[⊗]

Abstract: Electronegatively substituted iron(III) porphyrin chlorides such as tetrakis(pentafluorophenyl)porphyrin react with iodosylbenzenes, peracids, hydroperoxides, and hydrogen peroxide in hydroxylic solvents to form a high-valent oxene that is capable of carrying out further oxidations. According to the yields and stereochemistry of epoxidations, the oxene is formed exclusively via a heterolytic mechanism. Structure–reactivity studies show evidence for continual changes in transition-state structure rather than a change of mechanism from heterolysis with peracids to homolysis with hydroperoxides, as had previously been proposed. These changes can be described by the coefficients $\partial Q/\partial pK_a$ or $\partial\beta_{1g}/\partial\sigma$ and $\partial\beta_{1g}/\partial pK_a$. The observed $\partial Q/\partial pK_a$ or $\partial\beta_{1g}/\partial\sigma$, as well as the increase in β_{1g} with increasing pK_a^{ROH} , can be interpreted with a reaction-coordinate diagram in which both catalyst and oxidant are varied. On the basis of the heterolytic mechanism, a method for efficient, catalytic, and stereoselective epoxidation using simple and inexpensive hydroperoxides has been developed.

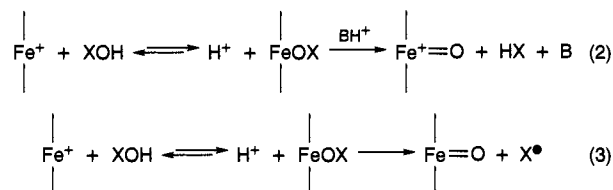
Introduction

The importance of iron(III) porphyrins in biological oxidations and their use as catalysts for synthesis have prompted extensive studies of their reactions with a variety of oxidants.^{1,2} Most of the kinetic studies have been carried out in hydroxylic solvents using either biomimetic hemins having a fifth, chelating imidazole ligand or synthetic iron(III) tetraarylporphyrins.^{3,4} These reactions use an oxidizing agent to create a reactive high-valent iron species that rapidly oxidizes the substrate (eq 1). The observed reaction is first order in oxidant and first order in catalyst. Kinetic studies of the dependence of the rate on the structure of the oxidant, the concentration of buffer, and the deuterium content of the solvent have been used to infer the mechanism of formation of the reactive oxidant.



Structure–reactivity studies have shown that stronger oxidants such as iodosylbenzenes and peracids react faster⁵ and that the reactions of peracids and hydroperoxides can be catalyzed by buffer^{3a,c} and by hydroxylic solvents.^{3d} These results have been taken as evidence for a heterolytic cleavage of the O–O bond and formation of an oxene (eq 2). (This is the π cation radical of an Fe(IV) species, for simplicity designated here as $\text{Fe}^+=\text{O}$). However, for hydroperoxides the mechanism has been more

controversial. Similar kinetic data from two different laboratories have been interpreted as supporting two mechanisms, either the same heterolytic cleavage (eq 2, $\text{X} = \text{RO}$)³ or else homolytic cleavage (eq 3, $\text{X} = \text{RO}$), to create an oxiron species, $\text{Fe}=\text{O}$, as the reactive oxidant.⁴



This dichotomy of interpretations might be resolved if conditions could be found such that all oxidants react by the same mechanism. We have recently shown that the electron-poor hemins iron(III) tetrakis(pentafluorophenyl)porphyrin chloride ((F₂₀TPP)FeCl) and iron(III) tetrakis(2,6-dichlorophenyl)porphyrin chloride ((TDCPP)FeCl) do react with pentafluoroiodosylbenzene, peracids, hydrogen peroxide, and *tert*-butylhydroperoxide exclusively by the heterolytic mechanism of eq 2.⁶ This series now makes it possible to establish a structure–reactivity relationship for this mechanism.

The evidence for operation of the heterolytic mechanism includes buffer catalysis, high yields, and high stereospecificity. Observations of acid catalysis⁷ and of catalysis by collidine buffers,^{3a,c} even with H₂O₂,^{4a,8} demonstrate the necessity for proton transfer as in eq 2, and they are not easily reconciled with homolytic cleavage (eq 3). This is not universal, since buffer catalysis is not always observed with ROOH⁹ and there is never acid/base catalysis by oxyanion bases, although it has

[†] Deceased, June 1993.

[⊗] Abstract published in *Advance ACS Abstracts*, March 15, 1995.

(1) *Cytochrome P-450: Structure, Mechanism and Biochemistry*; Ortiz de Montellano, P. R., Ed.; Plenum Press: New York, 1986.

(2) Mansuy, D. *Pure Appl. Chem.* **1987**, *59*, 759. Meunier, B. *Chem. Rev.* **1992**, *92*, 1411.

(3) (a) Traylor, T. G.; Lee, W. A.; Stynes, D. V. *J. Am. Chem. Soc.* **1984**, *106*, 755. (b) Traylor, T. G.; Lee, W. A.; Stynes, D. V. *Tetrahedron* **1984**, *40*, 553. (c) Traylor, T. G.; Ciccone, J. P. *J. Am. Chem. Soc.* **1989**, *111*, 8413. (d) Traylor, T. G.; Xu, F. *J. Am. Chem. Soc.* **1990**, *112*, 178.

(4) (a) Bruice, T. C. *Acc. Chem. Res.* **1991**, *24*, 243. (b) Gopinath, E.; Bruice, T. C. *J. Am. Chem. Soc.* **1991**, *113*, 4657, 6090.

(5) Traylor, T. G.; Marsters, J. C., Jr.; Nakano, T.; Dunlap, B. E. *J. Am. Chem. Soc.* **1985**, *107*, 5537.

(6) (a) Traylor, T. G.; Tsuchiya, S.; Byun, Y.-S.; Kim, C. *J. Am. Chem. Soc.* **1993**, *115*, 2775. (b) Traylor, T. G.; Fann, W.-P.; Bandyopadhyay, D. *J. Am. Chem. Soc.* **1989**, *111*, 8009.

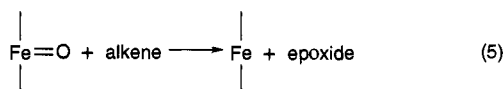
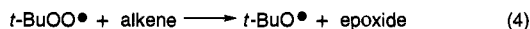
(7) Groves, J. T.; Watanabe, Y. *J. Am. Chem. Soc.* **1988**, *110*, 8443. (8) Zippies, M. F.; Lee, W. A.; Bruice, T. C. *J. Am. Chem. Soc.* **1986**, *108*, 4433. Panicucci, R.; Bruice, T. C. *J. Am. Chem. Soc.* **1990**, *112*, 6063.

(9) Lindsay Smith, J. R.; Balasubramanian, P. N.; Bruice, T. C. *J. Am. Chem. Soc.* **1988**, *110*, 7411. Balasubramanian, P. N.; Lee, R. W.; Bruice, T. C. *J. Am. Chem. Soc.* **1989**, *111*, 8714.

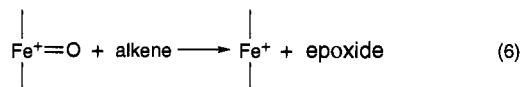
been noted^{3a} that buffer catalysis requires a base that does not bind to iron. We presume that even those that show no buffer catalysis react by the same heterolytic mechanism but with proton transfer primarily from lyonium ion to FeOOR, which is kinetically indistinguishable from the observed behavior.

A low yield of epoxidation products from hydroperoxides and hydrogen peroxide is evidence for the presence of radicals, which initiate chain decomposition of the peroxide. Thus the ability to obtain high-yield epoxidations^{6a} with (F₂₀TPP)FeCl or (TDCPP)FeCl and hydrogen peroxide or *tert*-butyl hydroperoxide is evidence for the absence of free radicals and thus for a heterolytic mechanism (eq 2).

Epoxidation itself is not conclusive for heterolytic cleavage (eq 2), since epoxidation might also be performed by peroxy radicals (eq 4) or by the oxoiron species (eq 5). However, two stereochemical aspects exclude epoxidation by either of these.^{6a} One is stereospecificity. For example, epoxidation of *cis*-stilbene with *tert*-butylperoxy radical gives a mixture of *cis* and *trans* epoxides because the intermediate *t*-BuOOCHPh-CHPh[•] undergoes rotation about the C-C bond before *t*-BuO[•] expulsion.¹⁰⁻¹³ Likewise, the oxoiron species shows no stereospecificity in epoxidation of β -methylstyrene.¹⁴ In contrast, epoxidation of *cis*-stilbene by the oxene derived from iodosylbenzenes is stereospecifically *syn*.¹⁵ Thus observation of *syn* epoxidation requires the oxene, whereas loss of stereospecificity is consistent with epoxidation by other species.

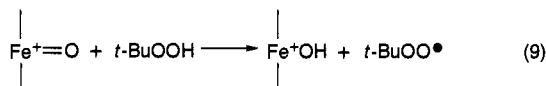
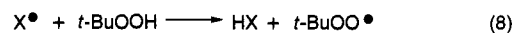
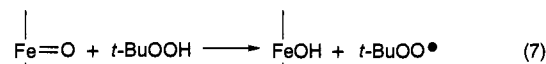


Stereoselectivity is also characteristic in each of these pathways. Epoxidation of norbornene with *tert*-butylperoxy radical produces only the *exo* epoxide.⁶ In contrast, the oxenes derived from (F₂₀TPP)FeCl or (TDCPP)FeCl afford mixtures of *exo* and *endo* epoxides in the ratios of 23:1 and 9:1, respectively. This ratio is characteristic not only of oxene epoxidation but also of the particular oxene. Thus since epoxidation of norbornene with hydrogen peroxide or *tert*-butyl hydroperoxide using (F₂₀TPP)FeCl again produces an *exolendo* ratio of 23:1,^{6a} it follows that epoxidation was effected by the oxene (eq 6). We maintain that the presence of the oxene requires heterolysis (eq 2), although it has also been suggested^{10b} that the oxene can arise by homolysis (eq 3) followed by oxidation of the oxoiron species by *t*-BuOOH. We cannot exclude this indirect mechanism, but it is surprising that such an oxidation would occur only with this electron-deficient heme.



It should be noted that the converse conclusion does not follow. Epoxidizing species other than the oxene do not necessarily arise by a homolytic pathway (eq 3, followed by eq

7 or eq 8). They can also arise by a heterolytic one (eq 2, followed by eq 9).¹⁶ Thus epoxidation could occur via peroxy radicals even though these do not necessarily arise from homolysis.



These observations show that all of the oxidants—iodosylbenzenes, peracids, *tert*-butyl hydroperoxide, and hydrogen peroxide—react with (F₂₀TPP)FeCl or (TDCPP)FeCl exclusively by heterolysis to produce the oxene. We are thus in a position to determine the effects of structural changes on rates of oxene formation. We now report that electron-withdrawing groups on the iron(III) porphyrin retard the reaction with pentafluoriodosylbenzene but accelerate the reaction with hydroperoxides. This surprising result is responsible for some of the kinetic observations¹⁷ that were offered as evidence for homolytic cleavage of hydroperoxides. We further show how these results are consistent with heterolytic cleavage of the O-O bond, and we present an interpretation of the effects of structural changes on rates.

Experimental Section

Materials. The following chemicals and solvents were used without further purification: sodium bicarbonate (Fisher), *trans*- β -carotene (Aldrich), cumene hydroperoxide (Aldrich, technical grade 80%), *tert*-butyl hydroperoxide (Aldrich, 70% in water), hydrogen peroxide (Aldrich, 30% in water), ethyl hydroperoxide (Polysciences, 10% in water), Oxone (HOOSO₃K, Alfa), iodopentafluorobenzene (Aldrich, 99%), dichloromethane (Fisher, spectra grade), and methanol (Fisher, spectra grade). 2,4,6-Tri-*tert*-butylphenol was recrystallized five times from ethanol-water (9:1) just prior to use. Norbornene (Aldrich) was distilled under argon. Dibromomethane (Aldrich) was distilled from calcium hydride under argon. 2-Butanone (Aldrich) was distilled from potassium carbonate. 3-Chloroperoxybenzoic acid (MCPBA, Fisher) was purified as previously described.¹⁸ Pentafluoriodosylbenzene (PFIB; *caution*, potentially explosive on heating¹⁹) and diphenylcyanomethyl hydroperoxide were prepared and purified using literature methods.²⁰ Purities of all oxidants were determined by iodometric analysis as previously described.^{3a}

Hemins. Iron(III) tetraphenylporphyrin chloride ((TPP)FeCl), iron(III) tetrakis(pentafluorophenyl)porphyrin chloride ((F₂₀TPP)FeCl), and iron(III) tetrakis(4-methoxyphenyl)porphyrin chloride were commercially available from Aldrich. The other substituted iron(III) tetraphenylporphyrin chlorides were obtained from previous studies.¹¹

Instruments. UV-visible spectra and kinetic runs were recorded at room temperature on a Kontron 810 spectrophotometer. Product analyses were performed on a Varian 3700 gas chromatograph equipped with a 10% Carbowax 20M 80/100 Supelcoport column.

Kinetic Methods. Oxygen Transfer from PFIB to Substituted Iron(III) Tetraphenylporphyrin Chlorides. The rates of intermediate formation from PFIB were obtained using pseudo-first-order rate

- (10) (a) Labeque, R.; Marnett, L. J. *J. Am. Chem. Soc.* **1989**, *111*, 6621. (b) He, G.-X.; Bruice, T. C. *J. Am. Chem. Soc.* **1991**, *113*, 2747.
 (11) Traylor, T. G.; Miksztal, A. R. *J. Am. Chem. Soc.* **1989**, *111*, 7443.
 (12) Groves, J. T.; Nemo, T. E.; Myers, R. S. *J. Am. Chem. Soc.* **1979**, *101*, 1032.
 (13) Collman, J. P.; Kodadek, T.; Brauman, J. I. *J. Am. Chem. Soc.* **1986**, *108*, 2588. Collman, J. P.; Brauman, J. I.; Meunier, B.; Hayashi, T.; Kodadek, T.; Raybuck, S. A. *J. Am. Chem. Soc.* **1985**, *107*, 2000.
 (14) Groves, J. T.; Gross, Z.; Stern, M. K. *Inorg. Chem.* **1994**, *33*, 5065.
 (15) Groves, J. T.; Nemo, T. E. *J. Am. Chem. Soc.* **1983**, *105*, 5786. Castellino, A. J.; Bruice, T. C. *J. Am. Chem. Soc.* **1988**, *110*, 158.

- (16) Traylor, T. G.; Xu, F. *J. Am. Chem. Soc.* **1988**, *110*, 1953.
 (17) (a) Lee, W. A.; Bruice, T. C. *J. Am. Chem. Soc.* **1985**, *107*, 513. (b) Lee, W. A.; Yuan, L.-C.; Bruice, T. C. *J. Am. Chem. Soc.* **1988**, *110*, 4277. (c) Bruice, T. C.; Balasubramanian, P. N.; Lee, R. W.; Lindsay Smith, J. R. *J. Am. Chem. Soc.* **1988**, *110*, 7890.
 (18) Schwartz, N. N.; Blumberg, J. H. *J. Org. Chem.* **1964**, *29*, 1976.
 (19) Collman, J. P. *Chem. Eng. News* **1985**, *63* 11, p 2.
 (20) Saltzman, H.; Sharefkin, J. G. *Organic Syntheses*; Wiley: New York, 1973; Vol. V, p 658. Selikson, J. J.; Watt, D. S. *J. Org. Chem.* **1975**, *40*, 267.

methods as previously reported.¹⁶ In a typical experiment, a solution of hemin (1.0×10^{-6} M) and *trans*- β -carotene (1.0×10^{-5} M) in 0.4 mL of $\text{CH}_2\text{Cl}_2/\text{CH}_3\text{OH}/\text{H}_2\text{O}$ (80:18:2 v/v) was prepared in a quartz cuvette (1 cm path length) equipped with a 2 in. neck sealed with a rubber septum. The reaction was initiated by adding 1–5 μL of a 1.0×10^{-4} M PFIB solution in the same solvent. The reaction was monitored by spectrophotometrically following the disappearance of *trans*- β -carotene at 468 nm ($\epsilon = 1.3 \times 10^5 \text{ M}^{-1} \text{ cm}^{-1}$). Some of the rate constants were determined by observing the disappearance of PFIB itself. Absorbance vs time curves indicated a pseudo-first-order reaction. Rate constants were evaluated from the average of the first 5 half-lives or from least-squares analysis of the linearized equations. Subsequent division by hemin concentration afforded the second-order rate constant, k_2 .

Oxygen Transfer from Peracids and Hydroperoxides to Substituted Iron(III) Tetraphenylporphyrin Chlorides. The rates of intermediate formation from these oxidants were obtained using the pseudo-first-order rate method described above. In a typical procedure, a quartz cuvette was charged with 0.5 mL of a $\text{CH}_2\text{Cl}_2/\text{CH}_3\text{OH}$ (25:75 v/v) solution of 2,4,6-tri-*tert*-butylphenol (0.07–0.2 M). The cuvette was sealed with a rubber septum, and appropriate amounts of concentrated hemin and 1:1 collidine/collidine hydrochloride solutions were injected to give the desired concentrations (10^{-4} M hemin when using hydroperoxides and 5×10^{-6} M when using peracids). The solution was then deoxygenated by bubbling with solvent-saturated argon for 10 min. To this solution was injected 1–10 μL of a concentrated hydroperoxide solution to initiate the reaction. (For peracids 1.5 mL of a 0.1 M solution of 2,4,6-tri-*tert*-butylphenol in the same solvent system was used, but the remainder of the reaction was carried out as described for hydroperoxides.) The reaction was monitored by spectrophotometrically following the pseudo-first-order production of 2,4,6-tri-*tert*-butylphenoxy radical. The rate constants were evaluated as described above.

Oxidations. Oxidation of Norbornene by Methylethyldioxirane (MED) with and without (TDCPP)FeCl. In a typical procedure, a two-phase mixture consisting of 1 mL of saturated aqueous NaHCO_3 and a solution of 0.05 M norbornene and 0 or 1.0 mM (TDCPP)FeCl in 1 mL of 2-butanone was briefly stirred. Oxone (0.1 equiv) was added, and the mixture was vigorously stirred for 20–30 min. An aliquot of the organic layer was then analyzed for oxidation products by GC. Product yields based on the amount of Oxone used were determined relative to an added standard of dibromomethane.

Oxidation of Norbornene by Methylethyldioxirane (MED) after Prior Incubation with and without (TDCPP)FeCl. A two-phase mixture consisting of 1 mL of saturated aqueous NaHCO_3 and 1 mL of 2-butanone containing (TDCPP)FeCl (0 or 1.2 mM) was cooled in an ice bath. Oxone (6.7 mg) was added, and the mixture was vigorously stirred in the ice bath for 15 min. A 2 M solution of norbornene in 0.5 mL of 2-butanone was added via syringe. Stirring was continued for 20 min, and an aliquot was removed and analyzed for products by GC. The remaining mixture was stirred for a total of 24 h, and another aliquot was analyzed for products. Product yields based on the amount of Oxone used were determined relative to an added standard of iodopentafluorobenzene.

Hemin-Catalyzed Epoxidation of Norbornene by PFIB. To a two-phase mixture consisting of norbornene (0.5 M) and (TDCPP)FeCl (0.001 M) in 0.5 mL of 2-butanone and 0.5 mL of saturated aqueous NaHCO_3 was added PFIB (1.5 mg, 0.01 M). The resultant mixture was vigorously stirred for 30 min at room temperature. An aliquot of the 2-butanone layer was then analyzed for oxidation products by GC. Product yields were determined relative to the iodopentafluorobenzene produced.

Results

Reactions of Pentafluoriodosylbenzene (PFIB). Rates of reaction of PFIB in its hydrated or methanolated form with various iron(III) porphyrin chlorides were determined by following the disappearance of β -carotene at 468 nm. Table 1 shows the hemins used and the second-order rate constants k_2 . The reactions were clearly pseudo first order, and the first-order rate constants were independent of β -carotene or pentafluor-

Table 1. Rate Constants (25 °C) for Reaction of PFIB with Substituted Iron(III) Tetraphenylporphyrin Chlorides in $\text{CH}_2\text{Cl}_2/\text{CH}_3\text{OH}/\text{H}_2\text{O}$ (80:18:2) Monitored by Oxidation of β -Carotene

porphyrin ^a	$\Sigma\sigma$	$k_2, \text{M}^{-1}, \text{s}^{-1}$
Cl_5	1.43	9.3×10^2
2,4-(CF_3) ₂	1.08	5.0×10^2
F_5	0.86	4.0×10^3
4-CN	0.66	9.1×10^3
2,6- Cl_2	0.46	2.0×10^3
4-Br	0.23	1.2×10^4
4-H	0.00	2.1×10^4
4-OCH ₃	-0.27	3.3×10^4
2,4,6-(CH_3) ₃	-0.51	1.07×10^4
4-N(CH_3) ₂	-0.83	9.1×10^4

^a Substituents on all four phenyl groups.

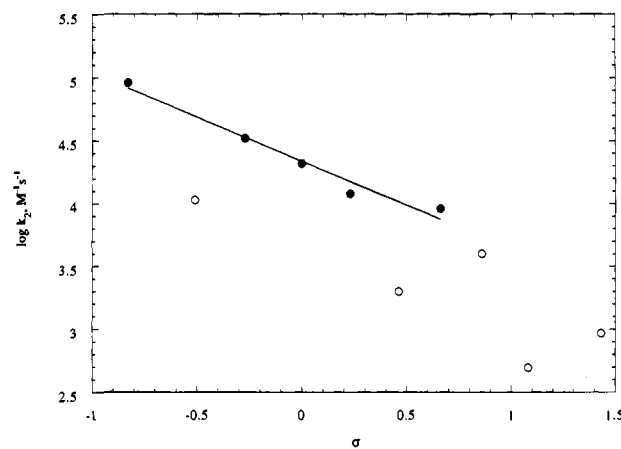


Figure 1. Substituent effects on reaction of various iron(III) porphyrins with PFIB, monitored by oxidation of β -carotene. Substituents as in Table 1. Ortho substituents (O) are omitted from the fit.

iodosylbenzene concentration. The data are plotted logarithmically in Figure 1 against the sum of σ values²¹ for the substituents. The σ values for substituents F_5 , Cl_5 , 2,4-(CF_3)₂, and 2,4,6-(CH_3)₃ are only estimates based upon the assumption that $\sigma_o = \sigma_p$. Without these points the correlation of $\log k_2$ with σ is very good. The slope is -0.70 , which clearly indicates that electron donation increases the rate.

Reactions of Peracids. Only two peracids were studied with three different hemins. The slope of a plot of $\log k_2$ vs σ (not shown) is near zero. It is clear that these rates depend little upon hemin structure.

Reactions of Hydrogen Peroxide and Hydroperoxides. The second-order rate constants for reactions of hydroperoxides with iron(III) porphyrins were determined by following the appearance of 2,4,6-tri-*tert*-butylphenoxy radical as previously described.^{3a,c,17a} Yields of the radical were 15 to 60%. The rate constants for reaction of various iron(III) porphyrins with *tert*-butyl hydroperoxide, plotted logarithmically against σ , are shown in Figure 2. The slope is ca. 0.4. Although the data are limited, it is clear that electron donation decreases the rate, in contrast to the effects on the PFIB reaction rates.

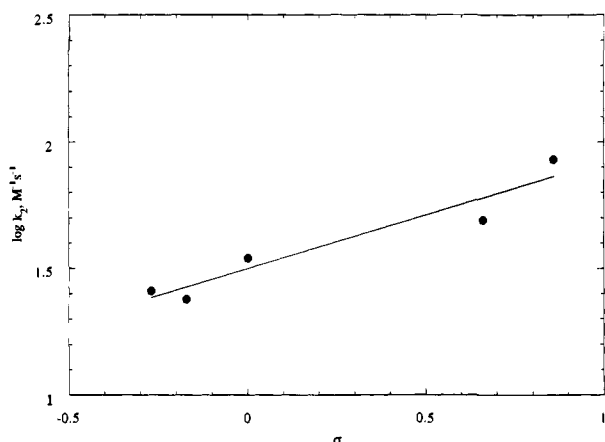
The rate constants for reaction of various hydroperoxides and peracids with (F_{20}TPP)FeCl are listed in Table 2. Most of these are from reactions in 25:75 $\text{CH}_2\text{Cl}_2/\text{CH}_3\text{OH}$, monitored by production of 2,4,6-tri-*tert*-butylphenoxy radical, but the same values are obtained in a 75:25 mixture, monitored by disappearance of β -carotene. These control experiments show that rates are not sensitive to solvent, and they verify that the rate being measured is the formation of the reactive oxidant. Additional control experiments show that the rates are not

(21) Lowry, T. H.; Richardson, K. S. *Mechanism and Theory in Organic Chemistry*, 3rd ed.; Harper and Row: New York, 1987; p 144.

Table 2. Rate Constants ($M^{-1} s^{-1}$) and Product Yields^a for the Reaction of Hydroperoxides and Peracids with $(F_{20}TPP)FeCl$ in Collidine-Buffered CH_2Cl_2/CH_3OH (25:75) Monitored by Production of 2,4,6-Tri-*tert*-butylphenoxy Radical

oxidant	[buffer], M						k_2^0 ^b
	0		1×10^{-3}		3×10^{-3}		
	k_2	% yield	k_2	% yield	k_2	% yield	
H_2O_2	190 ± 25 ^c	55 ± 3	188 ± 7	34.7 ± 0.7	190 ± 12	35.7 ± 0.4	93 ^d
<i>t</i> -BuOOH	77 ± 15 ^e	39 ± 1	119 ± 2.5 ^f	35.1 ± 0.3	185 ± 8	36.5 ± 1.6	86
EtOOH	77 ± 1	30.0 ± 0.3	77.5 ± 3	28 ± 1			77
$PhC(CH_3)_2OOH$	30 ± 2 ^g	38 ± 1	86.8 ± 3.5	34.5 ± 0.7	150 ± 3	33.1 ± 0.7	55
$Ph_2C(CN)OOH$	97 ± 11	16 ± 1	117 ± 2	18.5 ± 0.8	197 ± 1	16.4 ± 0.1	77
MCPBA	$(2.9 \pm 0.3) \times 10^3$	~100	$(3.4 \pm 0.2) \times 10^3$	~100	$(6.2 \pm 0.3) \times 10^3$	~100	2.1×10^3
$C_{11}H_{23}CO_3H$	$(1.3 \pm 0.3) \times 10^3$	86 ± 5	$(1.4 \pm 0.6) \times 10^3$	85 ± 4	$(1.96 \pm 0.02) \times 10^3$	84.5 ± 0.1	1.1×10^3

^a Phenoxy radical yield, based on oxidant. ^b Intercept of k_2 vs collidine concentration. ^c $191 M^{-1} s^{-1}$ for reaction in $CH_2Cl_2/MeOH$ (75/25) monitored by oxidation of β -carotene. ^d Statistically corrected. ^e $71 M^{-1} s^{-1}$ for reaction in $CH_2Cl_2/MeOH$ (75/25) monitored by oxidation of β -carotene. ^f Unchanged in the presence of 0.005 or 0.01 M tetrabutylammonium perchlorate. ^g $230 M^{-1} s^{-1}$ for reaction with chelated protohemin chloride in methanol.

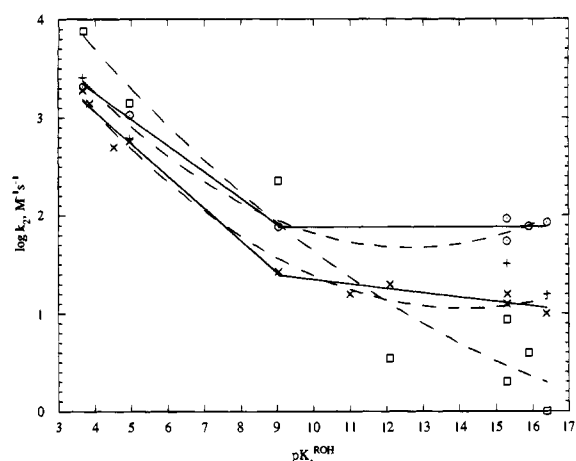
**Figure 2.** Substituent effects on reaction of various iron(III) porphyrins by *tert*-butyl hydroperoxide, monitored by oxidation of 2,4,6-tri-*tert*-butylphenol. Substituents from left to right are 4-OCH₃, 4-CH₃, H, 4-CN, F₅.

subject to salt effects. In Figure 3 the rate constants for the various ROOH are plotted logarithmically vs the pK_a of the corresponding ROH. Also included are rate constants for three other porphyrins. For consistency in comparing various studies, rates in buffers are extrapolated to zero buffer concentration, and such extrapolated rate constants are also included in Table 2.

Reactions of Methylethyldioxirane. Results are given in Table 3. As reported,²² reaction of methylethyldioxirane with norbornene affords good yields of the *exo* epoxide, but <0.1% of the *endo* isomer. Additionally, incubation of the Oxone/2-butanone mixture with iron(III) tetrakis(2,6-dichlorophenyl)porphyrin chloride ($10^{-3} M$) for 15 min, a time long enough for the dioxirane to be generated, did not lead to bleaching of the porphyrin. Addition of norbornene to this mixture and stirring the mixture at room temperature produced the *exo* epoxide with no trace of the *endo*, in yields comparable to the reaction without hemin. These observations, and those previously reported,²³ show that dioxiranes do not react with iron(III) porphyrins.

Discussion

Proton Transfers. The heterolytic mechanism involves deprotonation of the peroxy reagent and proton transfer to assist loss of a poor leaving group. Yet it is clear from the pH dependence of the rate constants in aqueous solution^{4b} that all the various protonation states of FeOOR can react, as well as those deprotonated from the ligand on Fe. Therefore it might seem as though dissociation of a proton from ROOH can occur

**Figure 3.** Plots of $\log k_2$ vs pK_a of ROH for reaction of various hemins with peracids and hydroperoxides ROOH, monitored by oxidation of 2,4,6-tri-*tert*-butylphenol catalyzed by (\square) chelated protohemin chloride in methanol, from ref 3c except for $Ph_2C(CN)OOH$ from Table 2, (\times) (TPP)FeCl in methanol from ref 17a, (+) (TDCPP)FeCl in $CH_2Cl_2/CH_3OH/H_2O$ (80:18:2), (\circ) ($F_{20}TPP$)FeCl in CH_2Cl_2/CH_3OH (25:75), extrapolated to zero collidine buffer. Peracids and hydroperoxides from left to right: MCPBA, $PhCO_3H$, $Cl(CH_2)_4CO_3H$, perlauric acid, $Ph_2C(CN)OOH$, $Ph_2C(COOCH_3)OOH$, Ph_3COOH , H_2O_2 , EtOOH, $PhC(CH_3)_2OOH$, *t*-BuOOH (not all for every series). Solid lines are fits to intersecting straight lines characteristic of a change of mechanism. Dashed lines are fits to a curve characteristic of a continuously varying mechanism.**Table 3.** Oxidation of Norbornene with Methylethyldioxirane (MED) and Pentafluoroiodosylbenzene (PFIB) in the Presence and Absence of (TDCPP)FeCl

oxidant	% epoxide ^a	exo/endo
MED (no prior incubation)	68	>1000
MED + (TDCPP)FeCl (no prior incubation)	68	>1000
MED (with prior incubation)	16	>1000
MED + (TDCPP)FeCl (with prior incubation)	14	>1000
PFIB + (TDCPP)FeCl	74	11 ^b

^a Based on oxidant (Oxone or PFIB). Except for the last entry, no other oxidation products were observed. ^b Same as under homogenous conditions in 2-butanone.

but is not required. However, mechanisms with proton transfer from H_3O^+ to FeOOR and with various states of protonation of the ligand on Fe are kinetically indistinguishable from the observed behavior.

A key piece of evidence for proton transfer in heterolytic cleavage is the observation of buffer catalysis, although this is not universal. For example, according to Table 2, neither H_2O_2 nor EtOOH shows buffer catalysis, but *t*-BuOOH does. The origin of this variability is uncertain, but it may arise from the

presence of water, inasmuch as these oxidants were introduced as 30%, 10%, and 70% solutions, respectively, in water. This may also account for the absence of buffer catalysis in aqueous solutions.⁹ To compare all the studies, rates are extrapolated to zero buffer concentration, and we view these rates as corresponding to proton donation from lyonium ion to FeOX.

Further evidence for the role of proton transfer comes from comparison with dioxiranes. If ROOH could coordinate to iron without deprotonation, then dioxirane should also. If the O—O bond of the coordinated ROOH can be cleaved without deprotonation, then so should that of dioxirane, the strongest oxidant used in this study, and with an O—O bond weakened by ring strain. That dioxirane does not react is consistent with a requirement for acid dissociation of the oxidant HOX and for formation of an FeOX precursor to the oxene (eq 2 or 3), as has been established for a variety of oxidants.^{3,7,24} The question we next address is whether the dissociation of the O—X bond is heterolytic (eq 2) or homolytic (eq 3).

Do Substituent Effects Indicate a Change of Mechanism?

Figure 3 shows contrasting substituent effects on rates of peracids and peroxides. When "chelated" protohemin, which bears an attached imidazole ligand, is the catalyst, the rates depend strongly on the structure of the oxidant.³ Yet in a subsequent study where iron(III) tetraphenylporphyrin chloride (TPPFeCl) was the catalyst, the rates again depend on peracid structure but they do not depend on hydroperoxide structure.¹⁷ The difference between chelated protohemin and TPPFeCl is not due to the difference in solvents since, as shown above, slight changes in solvent have little effect on rates. The observed break in the plot of $\log k_2$ vs pK_a^{ROH} at pK 9 was interpreted as evidence for a change of mechanism from heterolysis with peracids to homolysis with hydroperoxides. This is a reasonable interpretation, since the rate of homolytic cleavage would be insensitive to pK_a^{ROH} . Similar results in aqueous solutions were interpreted similarly.^{4,8,17c} Now a third set of data in Figure 3 provides a further contrast that permits a test of this interpretation.

In the Introduction we have summarized some of the evidence that both $(F_{20}\text{TPP})\text{FeCl}$ and $(\text{TDCPP})\text{FeCl}$, with electron-withdrawing groups, react by heterolysis with all oxidants, including hydrogen peroxide and *tert*-butyl hydroperoxide. We therefore can define the substituent effects for the pure heterolytic reaction. The plots of $\log k_2$ vs pK_a^{ROH} for these two catalysts are also shown in Figure 3. Clearly the oxidation with $(F_{20}\text{TPP})\text{FeCl}$ shows at least as prominent a break as does TPPFeCl. Therefore the observation of such a break is not necessarily an indication of a change to homolysis. Below we offer a reinterpretation of the break that is consistent with heterolysis.

If these breaks, which were taken as evidence for homolysis (eq 3), are actually characteristic of the heterolytic process (eq 2), the same may be true of the other evidence that has been claimed to support the homolytic mechanism:^{4,17} (1) production of *tert*-butoxy radicals and then acetone,^{4a} (2) low yields of epoxide,^{4a} (3) loss of stereospecificity in epoxidation,¹⁰ and (4) formation of the oxoiron species during the reaction.^{4a} Yet unlike the unequivocal case for heterolysis, which is based upon epoxide stereochemistry, all this evidence is indirect. It shows that there are radicals present, but it does not require that they

arise by homolysis of FeOOR. We have recently shown^{6a,25} that the first three of these results arise instead from reaction of *tert*-butyl hydroperoxide with the oxene species (eq 9), even when produced with either pentafluoriodosylbenzene or MCPBA. The loss of stereospecificity and the low yield are due to epoxidation by *tert*-butylperoxy radicals, which is both nonstereospecific and inefficient. We conclude that not only the kinetic evidence but also all of the other evidence presented for homolysis of hydrogen peroxide and *tert*-butyl hydroperoxide is consistent with heterolysis. The production of radicals, the low yields of epoxide, and the loss of stereospecificity are simply the results of a side reaction that can be avoided.

Structure—Reactivity Relations. In this paper we have established that O—O cleavage is heterolytic for all oxidants, and we now suggest that the transition state undergoes a change in structure. Changes in the slopes of structure—reactivity correlations often arise from variations in transition-state structure.²⁶ Comparison of Figures 1 and 2 shows that the sensitivity of the reaction rate to the substituents on the phenyl groups of hemins changes with the basicity of the leaving group. As pK_a^{ROH} decreases, ρ decreases from 0.4 for *t*-BuOOH (Figure 2) to ~ 0 for MCPBA (not shown). It decreases further to -0.8 for PFIB (Figure 1), whose pK_a^{ROH} is uncertain although it can be estimated as < 2 , since the pK_a of $\text{ArI}(\text{OH})_2$ is about 2,²⁷ and removing an oxygen should decrease the pK_a corresponding to the leaving group ArIOR^- , as in *m*-chlorobenzoic acid compared to *m*-chloroperbenzoic acid. These changes in ρ can be described by the coefficient $\partial\rho/\partial pK_a$ (eq 10), which is > 0 . Alternatively, the slopes in Figure 3 vary with the substituents on the phenyl groups of the hemin. With the electron-withdrawing $(F_{20}\text{TPP})\text{FeCl}$, the slope $\beta_{1g} = \partial \log k/\partial pK_a$ is less negative, or $\partial\beta_{1g}/\partial\sigma > 0$. Equation 10, relating both partial derivatives to the same mixed second partial derivative, shows that this increase of β_{1g} with increasing σ is complementary to the increase of ρ with pK_a .

$$\partial\rho/\partial pK_a = \partial^2 \log k/\partial pK_a \partial\sigma = \partial\beta_{1g}/\partial\sigma \quad (10)$$

The transition states for these reactions involve mainly bond breaking to the leaving group but also include significant proton transfer from an acid catalyst to the leaving group.³ It is convenient to interpret the changes in slopes (eq 10) with a reaction-coordinate diagram (Figure 4). The vertical axis represents proton transfer, the horizontal axis represents O—O bond cleavage, and an energy surface in the third dimension is to be understood.²⁶ Reaction proceeds from bottom left to top right, except for PFIB, where product is at the bottom right corner. The reaction coordinate is diagonal (solid line), with a transition state near the middle. The extent of proton transfer at the transition state is measured by the Brønsted coefficient α , and the extent to which positive charge is developed on the hemin is measured by the Hammett coefficient $-\rho$. Also β_{1g} , which measures the (positive) charge on the leaving group, increases from bottom right to top left.

An increase in basicity of the leaving group increases the energy of the bottom right corner relative to the top left corner. As a result the transition state will move downhill toward the upper left corner (perpendicular to the reaction coordinate, an

(25) Traylor, T. G.; Kim, C.; Fann, W.-P.; Perrin, C. L. Manuscript in preparation.

(26) Jencks, W. P. *Chem. Rev.* **1985**, *85*, 511. Alunni, S.; Jencks, W. P. *J. Am. Chem. Soc.* **1980**, *102*, 2052. Bourne, N.; Williams, A. *J. Am. Chem. Soc.* **1984**, *106*, 7591. Hupe, D. J.; Wu, D. *J. Am. Chem. Soc.* **1977**, *99*, 7653. Gandler, J. R.; Jencks, W. P. *J. Am. Chem. Soc.* **1982**, *104*, 1937. Young, P. R.; Jencks, W. P. *J. Am. Chem. Soc.* **1979**, *101*, 3288.

(27) Huheey, J. E. *Inorganic Chemistry*, 3rd ed.; Harper and Row: New York, 1983; p 297.

(22) Murray, R. W.; Jeyaraman, R. *J. Org. Chem.* **1985**, *50*, 2847.

(23) Wolowiec, S.; Kochi, J. K. *J. Chem. Soc., Chem. Commun.* **1990**, 1782.

(24) Baek, H. K.; Van Wart, H. E. *Biochemistry* **1989**, *28*, 5714. Jones, P.; Dunford, H. B. *J. Theor. Biol.* **1977**, *69*, 457. Yamaguchi, K.; Watanabe, Y.; Morishima, I. *Inorg. Chem.* **1992**, *31*, 156.

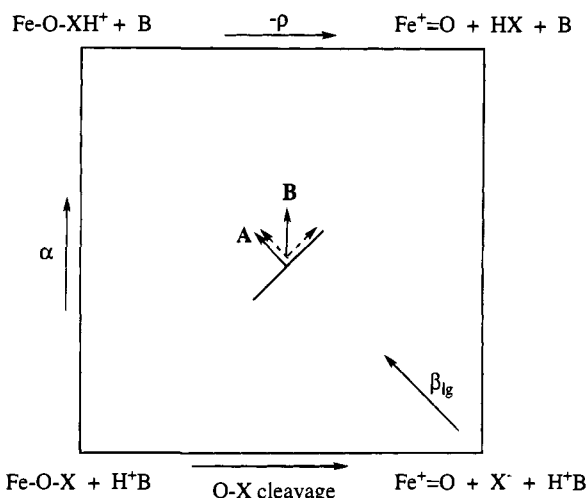


Figure 4. Reaction-coordinate diagram for the reaction of substituted hemin chlorides with various oxidants, with separate axes for proton transfer and O–X bond cleavage. Charge development on the iron atom is measured by ρ along the horizontal axis, and β_{1g} is measured along the diagonal axis. Energy contours are omitted.

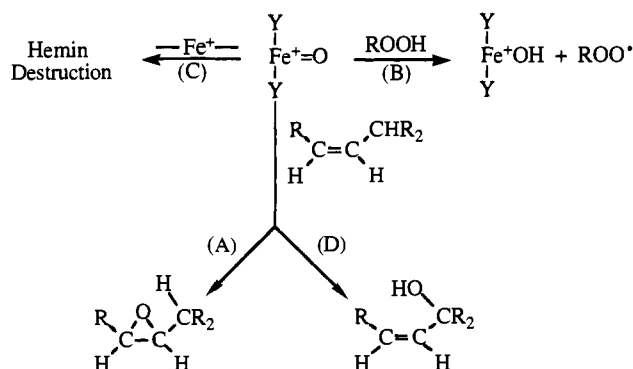
“anti-Hammond effect”), as indicated by arrow A in Figure 4. This corresponds to a transition state with less positive charge developed or a larger ρ . Thus $\partial\rho/\partial pK_a$ is >0 , as observed. Similarly, electron-withdrawing substituents on the hemin phenyl groups increase the energy of the right edge relative to the left. The transition state will move downhill toward the upper left corner (perpendicular to the reaction coordinate, an “anti-Hammond effect”) and also move uphill toward the upper right corner (parallel to the reaction coordinate, a “Hammond effect”). The result of these moves, shown as dotted arrows in Figure 4, is arrow B, toward the top, corresponding to a less negative value of β_{1g} . Thus $\partial\beta_{1g}/\partial\sigma$ is also >0 , as observed. A further prediction is that the Brønsted α for general acid catalysis increases with pK_a^{ROH} or with σ .

The dependence of the rate on the pK_a of ROH does not necessarily show a break. Instead we propose that it follows a smooth curve, as suggested by the dashed lines in Figure 3, including the data for chelated protohemin, where the curvature is less. The curvatures mean that the slope β_{1g} becomes less negative with increasing pK_a , corresponding to a positive value for the coefficient $\partial\beta_{1g}/\partial pK_a$ or $\partial^2 \log k/\partial pK_a^2$. As above, an increased pK_a^{ROH} moves the transition state toward the upper left corner (arrow A in Figure 4). This corresponds to a greater extent of proton transfer to the leaving group in the transition state, or an increased β_{1g} . Thus $\partial\beta_{1g}/\partial pK_a$ is >0 , observed as upward curvature in Figure 3. It should be noted that this curvature is opposite to the usual reactivity–selectivity relationship, which is evidence that it arises from the “anti-Hammond effect”, moving the transition state perpendicular to the reaction coordinate. Indeed, such curvature is to be expected for the heterolytic mechanism, and there is no break associated with a change of mechanism.

High-Yield Epoxidations with Hydroperoxides. How can high-yield, regioselective, and stereospecific epoxidations be achieved using hydroperoxides? The answer is that it is necessary to avoid the reaction of the oxene with the hydroperoxide (eq 9), since this competes with epoxidation. We can now examine those factors that might favor epoxidation so as to determine precautions to prevent the side reactions.^{4a,6a}

Some of the possible side reactions are shown in Scheme 1. The obvious first remedy is to use a high ratio of alkene to hydroperoxide, although this is often not sufficient.^{10a,28} Most importantly, we have found that as the substituents (Y) on the

Scheme 1. Reactions of Oxenes



porphyrin are made more electronegative, k_A/k_B , the ratio of the rate of epoxidation process A to that of process B, changes drastically. Even though electron-withdrawing substituents presumably increase both k_A and k_B , they increase k_A more and make the reaction more selective for alkene, perhaps because k_A corresponds to a two-electron reduction and k_B only a one-electron reduction of the oxene. For example, with iron(III) tetrakis(mesityl)porphyrin chloride $k_A/k_B \approx 0.01$ for cyclic alkenes and *t*-BuOOH; this ratio increases to >1 for $(\text{F}_{20}\text{TPP})\text{FeCl}$ and increases even more for perhalohemins.^{6a,29} Moreover, accompanying this change is an increase in k_A/k_C as the stability of the catalyst increases, as well as an increase in k_A/k_D , the selectivity for epoxidation. Therefore, by using electron-deficient iron(III) porphyrins in inert hydroxylic solvents, high yields of epoxide can be achieved with hydrogen peroxide.⁶ It should be noted that this is an impossibility according to the proposal of homolytic cleavage.

Other Hydroperoxides and Remaining Problems. We cannot conclude that all FeOOR must cleave heterolytically, even though we have questioned the previous evidence for homolytic cleavage. There is a class of hydroperoxides— $\text{RCH}=\text{CHCH}_2\text{CHR}'\text{OOH}$,^{10a,30} 2,6-di-*tert*-butyl-4-hydroperoxy-4-methyl-2,5-cyclohexadienone,^{31,32} and $\text{PhCH}_2\text{C}(\text{CH}_3)_2\text{-OOH}$ ³³—which are precursors to fragmenting alkoxy radicals and which do not appear to react by heterolysis even according to some of the criteria discussed here. For example, we have obtained only 20% cyclooctene epoxide using $\text{PhCH}_2\text{C}(\text{CH}_3)_2\text{-OOH}$ and $(\text{F}_{20}\text{TPP})\text{FeCl}$ as catalyst. However, catalytic epoxidation of norbornene with this peroxide does afford a 26:1 ratio of *exo* and *endo* epoxides,³³ consistent with oxene formation. This system is currently under investigation.

Conclusions

We have shown that electronegatively substituted iron(III) porphyrin chlorides such as tetrakis(pentafluorophenyl)porphyrin react with oxidants, including iodobenzene, peracids, hydroperoxides, and hydrogen peroxide, to form an oxene species via a heterolytic process. Evidence for this includes buffer catalysis and the high yields and stereospecificity of epoxidation of alkenes. That dioxiranes do not generate the oxene species makes the requirement for a predissociation of the oxidant acid

(28) Traylor, T. G.; Xu, F. *J. Am. Chem. Soc.* **1987**, *109*, 6201.

(29) Traylor, T. G.; Tsuchiya, S. *Inorg. Chem.* **1987**, *26*, 1338.

(30) Labeque, R.; Marnett, L. *J. Biochemistry* **1988**, *27*, 7060.

(31) Thompson, J. A.; Yumibe, N. P. *Drug Metab. Rev.* **1989**, *20*, 365. Yumibe, N. P.; Thompson, J. A. *Chem. Res. Toxicol.* **1988**, *1*, 385.

(32) Allentoff, A. J.; Bolton, J. L.; Wilks, A.; Thompson, J. A.; Ortiz de Montellano, P. R. *J. Am. Chem. Soc.* **1992**, *114*, 9744.

(33) Kim, C. Unpublished results.

and the subsequent formation of a hemin-oxidant precursor to the oxene clear. Also, it is now clear that most, if not all, of the evidence for a homolytic process can be interpreted in terms of the heterolytic reaction, including the formation of radicals during the oxidation process.

The characteristics of the heterolytic process could be defined through structure-reactivity studies in which both catalyst and oxidant were varied. For the reaction with pentafluoriodobenzene, electron-withdrawing substituents on the catalyst decrease the rate of reaction ($\rho < 0$). With hydroperoxides and hydrogen peroxide, electron withdrawal increases reactivity ($\rho > 0$), and there is little effect of catalyst structure on the rate of reaction with peracids ($\rho \approx 0$). This change is described by the coefficient $\partial\rho/\partial pK_a = \partial\beta_{1g}/\partial\sigma$. It is evidence for a change

in transition-state structure during heterolytic cleavage, which can be interpreted with a reaction-coordinate diagram. The upward curvature in the plots of $\log k_2$ vs pK_a^{ROH} corresponds to the coefficient $\partial\beta_{1g}/\partial pK_a$. This too can be attributed to a change in transition-state structure on a reaction-coordinate diagram. Finally, a method for efficient, catalytic, and stereoselective epoxidations using simple and inexpensive hydroperoxides in inert hydroxylic solvents has been developed.

Acknowledgment. We are grateful to the National Institutes of Health (T.G.T., Grant HL 13581) and the National Science Foundation (T.G.T., Grant CHE 87-21364) for support.

JA940711V